Electronic Supplementary Material (ESI) for Journal of Materials Chemistry C.

Supplementary Information

Suppressed ion migration in powder-based perovskite thick films using an ionic liquid

Philipp Ramming[1], Nico Leupold[2], Konstantin Schötz[1], Anna Köhler[1], Ralf Moos[2], Helen Grüninger[3], Fabian Panzer[1*]

[1] Soft Matter Optoelectronics, University of Bayreuth, Bayreuth 95440, Germany.

[2] Department of Functional Materials, University of Bayreuth, Bayreuth 95440, Germany

[3] Institute for Molecules and Materials, Radboud University, Heyendaalseweg 135, 6525 AJ Nijmegen, The Netherlands

Corresponding Author:

[*]E-Mail: fabian.panzer@uni-bayreuth.de

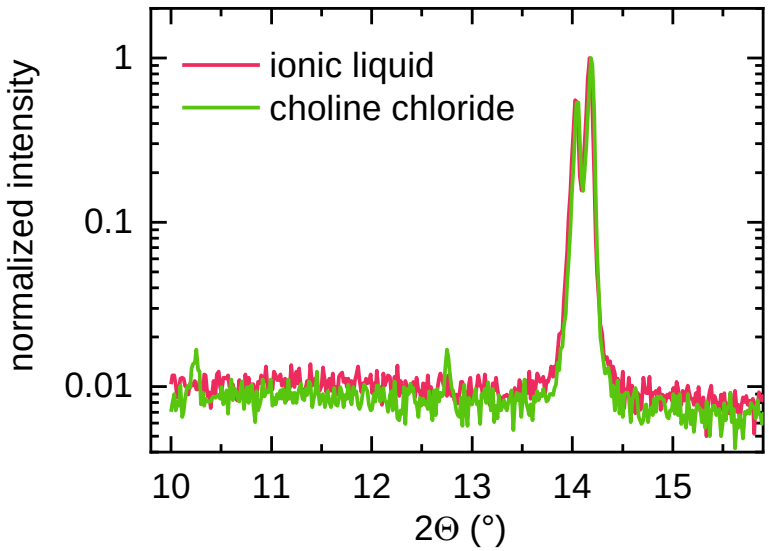

Fig. S1: XRD pattern of mechanochemically synthesized $MAPbI_3$ powders containing the ionic liquid $BMIMBF_4$ (red) or the solid organic salt choline chloride (green). In contrast to the pattern of the powder that contains IL, the pattern of the powder that contains choline chloride shows two additional peaks at 10.2° and 12.6°.

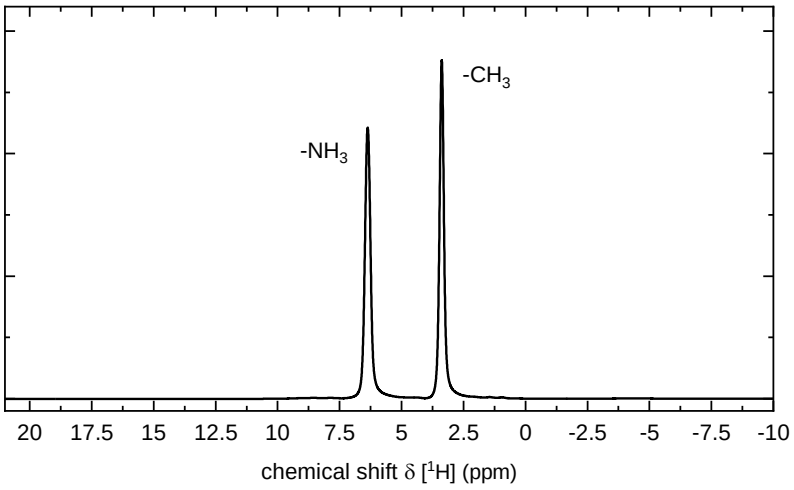

Fig. S2: ^{1}H NMR spectrum of the passivated $MAPbI_3$ powder containing ionic liquid. The two predominantly visible peaks originate from the $-NH_3$ and $-CH_3$ groups of the methylammonium cations within the perovskite. The signal from the ionic liquid is shown in a zoomed version of this data in Fig. 1 in the main text.

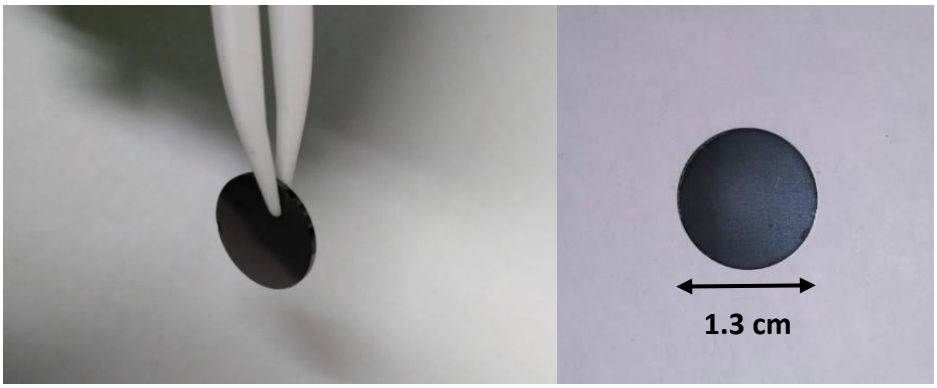

Fig. S3: The pressed thick films were obtained by pressing 0.4 g of the dry perovskite powder with 100 MPa on a homemade mechanical press. The diameter of the free-standing pellets is 1.3 cm and the thickness is about 0.8 mm. The density of the pellets therefore is about (3.75±0.05) g/cm^3.

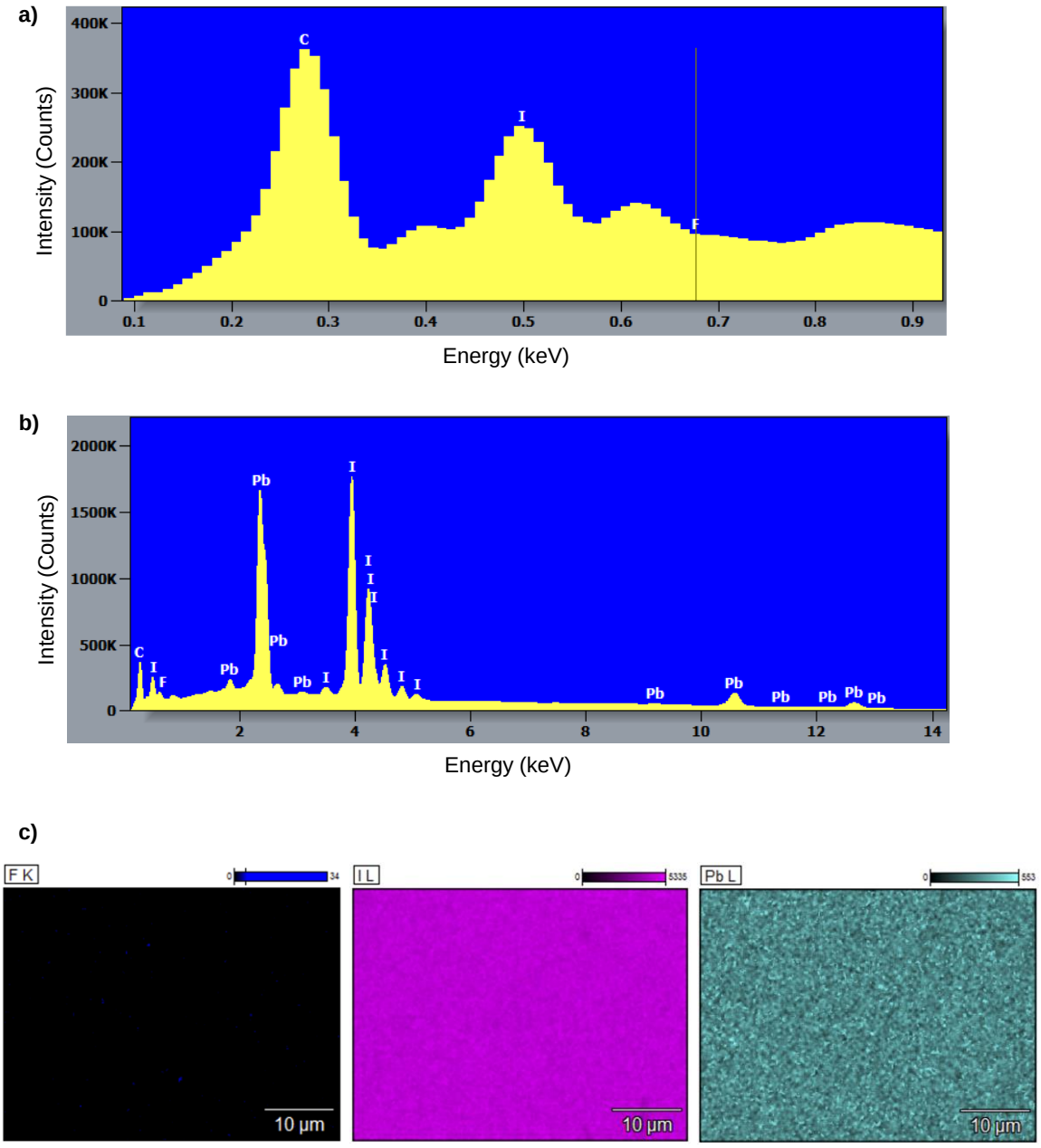

Fig. S4: (a) EDX spectrum obtained by mapping over the surface of the ionic liquid containing pellet surface. The positions of the K line of fluorine (F) is indicated by a vertical line. For fluorine that is only contained in the ionic liquid, there is no signal peak visible above the background. (b) Full EDX spectrum containing the L line of iodine (I) and lead (Pb), that are used for the mapping, at 3.94 keV and 10.55 keV respectively (c) The single element map of fluorine (F K) show almost no counts above the background threshold and no spots of local aggregations on the surface are detectable. The single element maps of iodine (I L) and lead (Pb L) are shown for comparison.

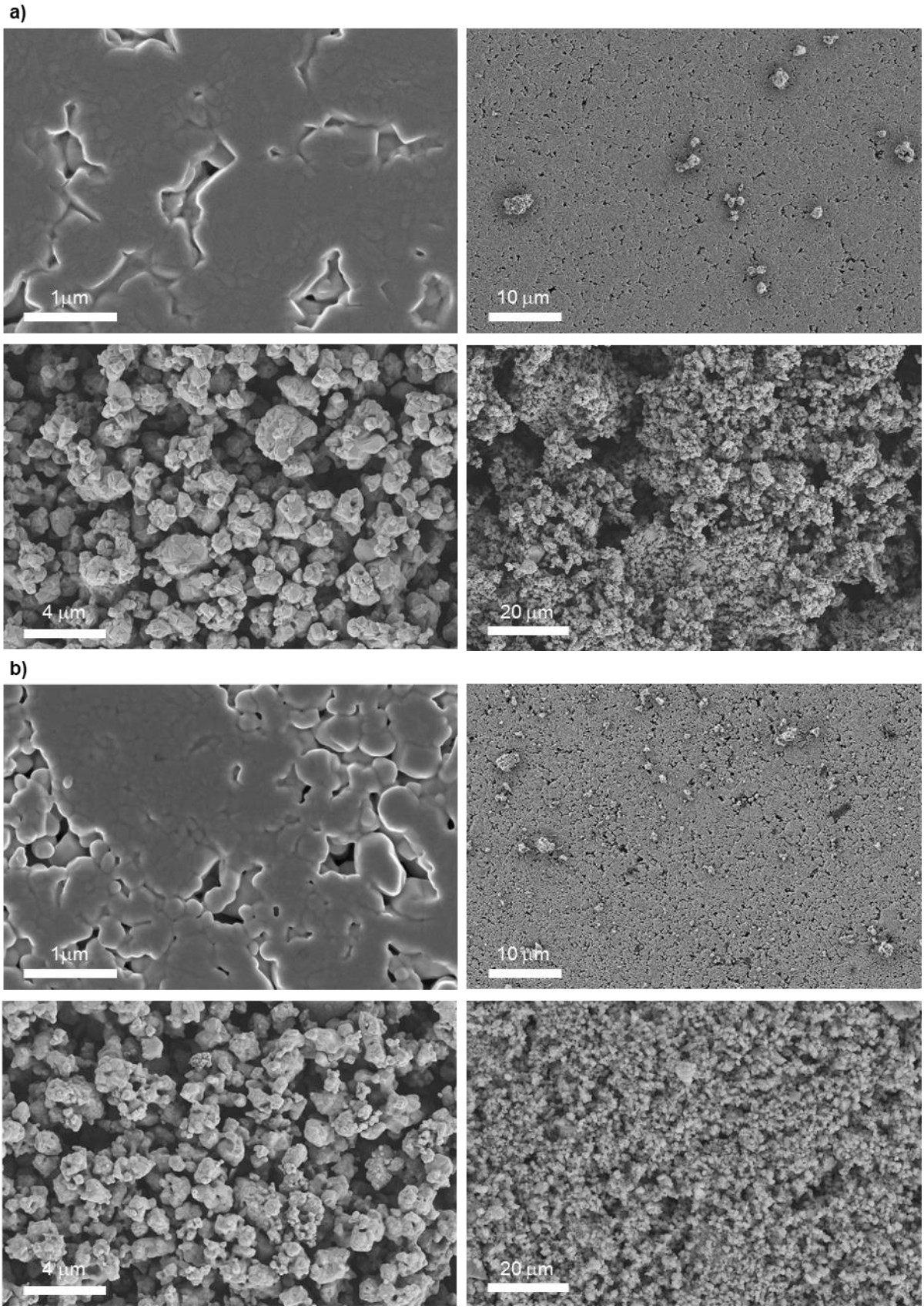

Fig. S5: (a) SEM images of the reference $MAPbI_3$ pellet surface (top) and reference powder (bottom). (b) SEM images of the passivated $MAPbI_3$ pellet (top) and passivated powder (bottom) containing ionic liquid.

Section S1 - Time resolved photoluminescence (TRPL):

As mentioned in the main manuscript, the charge carrier recombination after laser excitation in lead halide perovskites can be described by a rate equation of the form[1]

$$\left(\frac{\mathrm{d}n}{\mathrm{d}t}\right)_{\mathrm{rec}} = -k_1 n - k_2 n^2 - k_3 n^3 \qquad \text{(S1)}$$

where k_1 is the rate constant for mono-molecular trap-related recombination, k_2 is the bi-molecular (radiative) recombination rate constant and k_3 is the Auger-recombination rate constant. k_2 and k_3 are material constants, whereas k_1 depends on the trap density. Eqn (S1) is an approximation for the case that the electron density is approximately equal to the hole density. However, even in this case, diffusion of charge carriers and photon reabsorption change the local charge carrier density additionally. To account for both effects, eqn (S1) can be rewritten as[2]

$$\frac{\mathrm{d}n}{\mathrm{d}t} = D\frac{\partial^2 n}{\partial z^2} - k_1 n - k_2 n^2 - k_3 n^3 + G_{\mathrm{reabs}} \qquad \text{(S2)}$$

with D being the diffusion constant for the charge carriers, z is the spatial position normal to the surface and G_{reabs} is the generation rate of charge carriers by photon reabsorption. Eqn (S2) is also sometimes written as[2]

$$\frac{\mathrm{d}n}{\mathrm{d}t} = D\frac{\partial^2 n}{\partial z^2} - k_1 n - k_2^{\mathrm{apparent}} n^2 - k_3 n^3 \qquad \text{(S3)}$$

where k_2^{apparent} implicitly contains the effect of photon recycling and is not a material constant anymore.

Diffusion and photon reabsorption can lead to a quick flattening of the charge carrier distribution,[2] so that shortly after excitation, diffusion is negligible and eqn (S1) is sufficient to describe the charge carrier recombination when k_2^{apparent} is used instead of k_2.

Further, it follows from eqn (S1) that for low n ($k_1 >> k_2 n + k_3 n^2$), the transient PL shows a mono-exponential decay with a decay constant of $2k_1$ (since only k_2 is radiative). That means that a reduction in trap density leads to an increased mono-exponential lifetime. Such low n are present either upon using low excitation fluences or after a sufficient time after the excitation. This mono-exponential decay does not depend on the choice of the initial charge carrier density or k_2^{apparent}.

For fitting our transient PL data, we simulated PL resulting from eqn (S1) and eqn (S3). To reduce the number of free parameters, we used $k_2^{apparent} = 6.8\times10^{-10}$ cm^3s^{-1} and $k_3 = 10^{-28}$ cm^6s^{-1}.[2] The order of magnitude of initial charge carrier density was estimated based on the excitation laser fluence to be on the order of $n_{init} = n(z=0, t=0) \approx 10^{16}$ cm^{-3}, and was allowed to vary slightly around this value. Within these limitations, it was possible to fit our transient PL data without explicitly considering diffusion of charge carriers. We recall that the mono-exponential decay, which contains information about k_1, is independent of the choice of k_2 and n_{init}, so that we expect k_1 to be reliably extracted by our fits. We also modelled the transient PL including diffusion, which lead to similar values of k_1, namely $k_{1,ref,diff} = 2.069\times10^7$ s^{-1} and $k_{1,pass,diff} = 3.248\times10^6$ s^{-1}. While this introduced an additional free parameter D and a larger variation of n_{init}, the shape of the simulated PL curves only changed little, as shown in Fig. S5. Since we were only interested in k_1, we thus chose to discuss the PL curves that were modelled without taking diffusion into account.

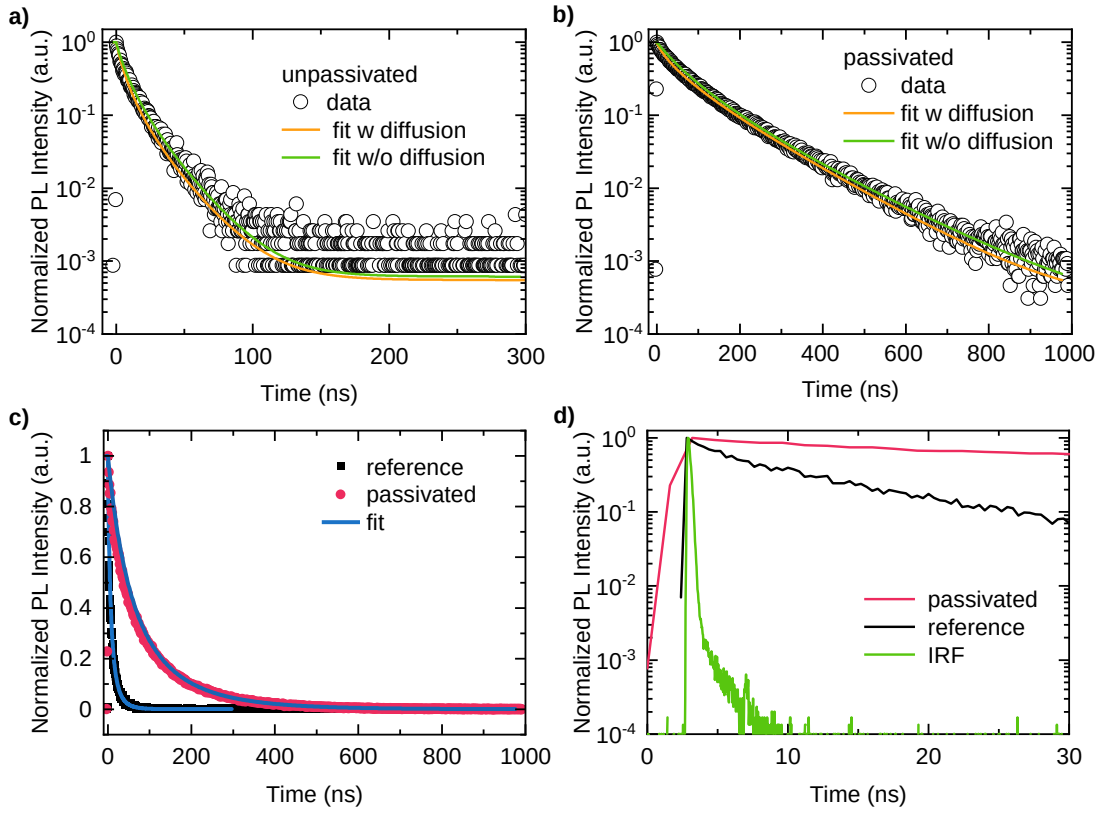

Fig. S6: Time-resolved PL for (a) the reference pellet and (b) the passivated pellet (black circles), together with modelled PL based on eqn (S1) and eqn (S2), i.e. without diffusion (green) and with diffusion (orange). (c) TRPL of the reference (red) and passivated (black) pellets with the corresponding fits without diffusion on a linear scale. (d) TRPL data of passivated (red) and reference (black) pellet together with the instrument response function (IRF, green).

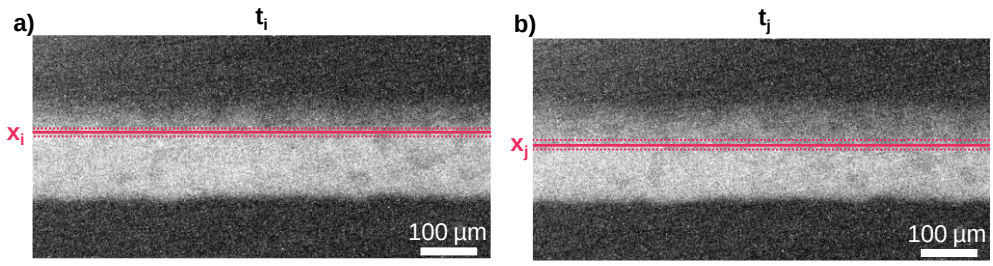

Fig. S7: Manual extraction of the position of the dark front from a series of PL images. Here two images at two different times t_i (a) and t_j (b) are shown with the dark front illustrated with a red line. The corresponding positions x_i and x_j were determined by determining the corresponding pixel line of the image and transforming it to a length with the help of the scalebar. The red dotted lines indicate the uncertainty of the dark front position.

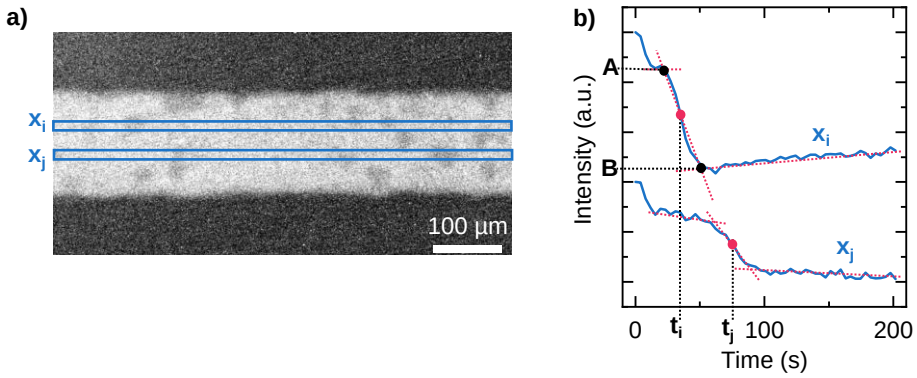

Fig. S8: Extraction of the position of the dark front by tracking the brightness within horizontal stripes along the channel. (a) Two horizontal stripes about 10 µm long at different positions along the channel (x_i and x_j) are indicated with blue boxes. (b) The average intensity in the region of the two stripes (x_i and x_j) in dependence of the time (blue lines, offset along intensity axis for clarity). We determined the times (t_i and t_j) at which the dark front passes the boxes at position x_i and x_j by determining the time at the center of the intensity step (red dots). The relative intensity drop that takes place with the dark front passing through the box is determined by taking the difference of the intensity before (black dot at A) and after (black dot at B) the front has passed and dividing the difference through the initial (A) intensity value (only shown here for the intensity drop in the box at x_i).

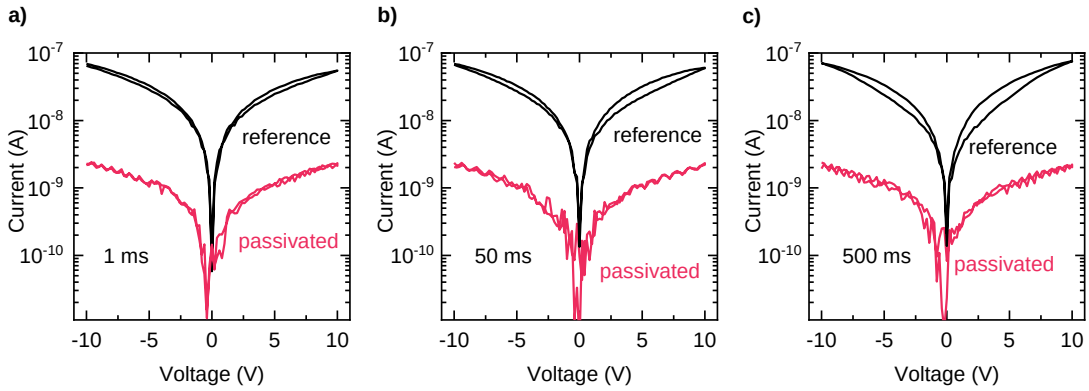

Fig. S9: Current-voltage characteristics with different holding times of each voltage step (1 ms, 50 ms, 500 ms). The measurement was conducted with lateral gold electrodes evaporated on top the reference (black curves) and passivated (red curves) pellets.

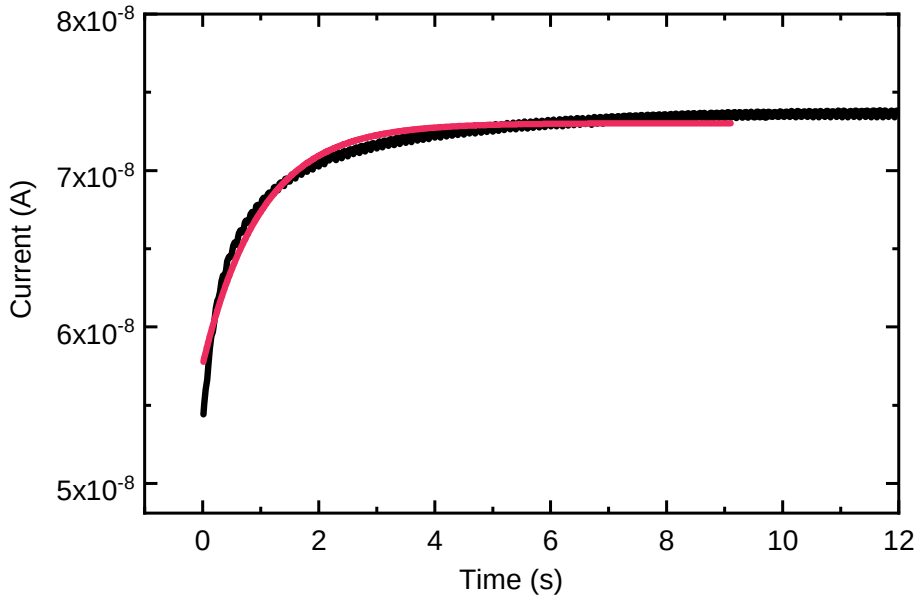

Fig. S10: Evolution of the dark current of the reference pellet (black line) within the first seconds after applying a voltage step of 10 V together with an exponential fit (red line), yielding a time constant of 1 s.

Supporting References:

1. L. M. Herz, *Annu. Rev. Phys. Chem.*, 2016, **67**, 65-89.
2. T. W. Crothers, R. L. Milot, J. B. Patel, E. S. Parrott, J. Schlipf, P. Müller-Buschbaum, M. B. Johnston and L. M. Herz, *Nano Lett.*, 2017, **17**, 5782-5789.